

# Abnormal microtubule packing in processes of Sf9 cells expressing the FTDP-17 V337M tau mutation

Thierry Frappier<sup>a</sup>, Nina S. Liang<sup>a</sup>, Kristy Brown<sup>a</sup>, Conrad L. Leung<sup>a</sup>, Timothy Lynch<sup>b</sup>, Ronald K.H. Liem<sup>a</sup>, Michael L. Shelanski<sup>a,\*</sup>

<sup>a</sup>Department of Pathology and Taub Center for Alzheimer's Disease Research, Columbia University College of Physicians and Surgeons, 630 West 168th Street, New York, NY 10032, USA

<sup>b</sup>Mater Private Hospital, Dublin 7, Ireland

Received 17 June 1999

**Abstract** Mutations in the gene for the microtubule associated protein, tau have been identified for fronto-temporal dementia with Parkinsonism linked to chromosome 17 (FTDP-17). In vitro data have shown that FTDP-17 mutant tau proteins have a reduced ability to bind microtubules and to promote microtubule assembly. Using the baculovirus system we have examined the effect of the V337M mutation on the organization of the microtubules at the ultrastructural level. Our results show that the organization of the microtubules is disrupted in the presence of V337M tau with greater distances between the microtubules and fewer microtubules per process.

© 1999 Federation of European Biochemical Societies.

**Key words:** Tau; FTDP-17; Baculovirus; V337M mutation

## 1. Introduction

The microtubule-associated protein tau is highly expressed in neurons, especially in axons, although it is also present in astrocytes and oligodendrocytes [1]. Tau promotes microtubule assembly and stability through a binding domain composed of either three or four imperfect repeats located near its C-terminus [2,3]. Accumulations of hyperphosphorylated tau are seen in Alzheimer's disease, where tau is the major component of the characteristic paired helical filaments (PHF), as well as in a variety of other dementing conditions including the fronto-temporal dementias with Parkinsonism (FTDP-17), progressive supranuclear palsy (PSP) [4-7] and familial subcortical gliosis [8].

Linkage analysis of kindreds with fronto-temporal dementias revealed that the gene responsible was located at or near the tau locus [9,10]. Further studies have identified a number of different dominant tau mutations in these families [9,11-14]. Some of these mutations are intronic and appear to affect the relative abundance of tau with four repeats versus tau with three repeats at its microtubule binding domain, while others are missense mutations in exons both within the microtubule binding domain coding region and outside of it. While these mutant forms of tau are all associated with FTDP-17, the manner in which tau contributes to the pathogenesis of the disease is not known. At present there is no evidence for any effect of these mutations on brain development and disease symptoms usually occur only after three or more decades of life. It is possible that this delayed expression is the end

result of accumulated damage from years of modest functional impairment of the neuronal cytoskeleton. Alternatively, it could be the direct result of the accumulation of abnormal tau aggregates in the cytoplasm.

In order to determine the properties of the tau proteins with FTDP-17 mutations, several recent in vitro studies have examined their ability to promote microtubule assembly [15,16], to bind to microtubules [15], to form fibrillar structures [17,18] and to induce alterations in physical and structural characteristics [19]. Although these studies differ in their details, in general the mutant tau proteins have altered the ability to promote microtubule assembly and to bind to microtubules, as well as altered conformations, and show a longer initial lag phase in microtubule polymerization. Furthermore, both a tau peptide containing one of the mutations, as well as recombinant proteins carrying any of a number of these mutations are more rapidly able to form fibrils than wild-type tau. Transfection studies have shown that tau with and without mutations binds to microtubules, but that the mutations reduced the length of microtubule extension in transfected cells [20]. In another report, the V337M mutation was found to disrupt the microtubule network in COS-7 cells [17]. The lack of ultrastructural data in these studies has obscured the nature of the disorganization and failed to suggest the mechanism(s) by which it occurs.

To determine how mutant tau affects microtubule organization, we have utilized the baculovirus expression system in the Sf9 insect cell line [21] and examined the processes resulting from the expression of these tau proteins at the EM level. The baculovirus inhibits host protein synthesis; viral proteins and 'foreign' genes under the control of the viral polyhedrin promoter are strongly expressed. When tau is expressed in these cells, there is formation of asymmetric microtubule-rich [22,23] processes. The organization of the microtubules in these processes is affected by the isoform of tau expressed. For example, low molecular weight (CNS) tau expression results in tighter microtubule packing than high molecular weight tau (PNS) and expression of tau without a projection domain results in even closer spacing [23].

In the studies reported here, we have prepared baculovirus constructs containing wild-type human tau and the V337M tau mutant to compare their expression and their effect on cytoskeletal organization in Sf9 cells.

## 2. Materials and methods

### 2.1. Preparation of tau cDNAs

Wild-type human tau cDNA was synthesized by PCR on adult human brain QUICK-Clone cDNA (Clontech, Palo Alto, CA,

\*Corresponding author. Fax: (1) (212) 305-5498.  
E-mail: mls7@columbia.edu

USA) using sense primer 5'-GGGACGTACGGGTTGGGGGACAGG-3' and antisense primer 5'-GGGCTGATCACAACCC-TGCTTG-3'. The resulting 1 kb PCR product was cloned into pCR2.1-TOPO (Invitrogen, Carlsbad, CA, USA) and sequenced in its entirety. The PCR product was found to correspond to the 412 amino acid four repeat isoform of human tau and was used as the template for creating the V337M mutation.

The V337M mutation was engineered by site directed mutagenesis using the primers 5'-GGGACGTACGGGTTGGGGGACAGG-3' and 5'-AAGCTTCTCAGATTTACTTCCATCTGGCC-3'. After PCR using wild-type human tau as a template, the PCR product was cloned in pCR2.1-TOPO (Invitrogen). The insert containing the mutant sequence was excised by *SacII* and *HindIII* and inserted in place of the wild-type human tau.

### 2.2. Generation of baculovirus constructs and baculovirus expression

Baculovirus constructs were made using the Bac-to-Bac baculovirus expression system (Life Technologies, Gaithersburg, MD, USA). In brief, human wild-type tau and the V337M tau mutation cDNAs were digested from the PCR2.1-TOPO vector by *EcoRI* and cloned in the *EcoRI* site of the pFASTBac1 shuttle vector. After amplification, DH10Bac bacteria were transformed with the recombinant vectors. After selection, recombinant viral DNAs were purified as described in the Bac-to-Bac protocol. Sf9 cells were transfected, according to the manufacturer's recommendations, with the recombinant viral DNA using the superfect transfection reagent (Qiagen, Valencia, CA, USA). Virus titers were determined both with end-point dilution and plaque assays.

### 2.3. Electron microscopy

Cells were fixed in 35 mm tissue culture dishes with 2.5% glutaraldehyde in 0.1 M Sorensen's buffer (pH 7.2) for 1 h. Cells were then rinsed and post-fixed with 1% OsO<sub>4</sub> in Sorensen's buffer for 30 min. After dehydration, cells were embedded in tissue culture dishes with a mixture of LX-112 (Ladd Research Industries Inc., Burlington, VT, USA) and EM-bed 812 (E.M.S., Fort Washington, PA, USA). The cells were removed from dishes and re-embedded on edge to ensure cross-section of processes. Thin Sections were cut on MT-700 RMC microtome, stained with uranyl acetate and lead citrate and examined using a JEM-1200 EXII JEOL microscope.

### 2.4. Protein purification and Western blot analysis

Three days after infection, Sf9 cells were collected by centrifugation for 10 min at 2000×g, washed twice with PBS, and then resuspended in reassembly buffer (0.1 M MES, 0.75 M NaCl, 0.5 mM MgSO<sub>4</sub>, 1 mM EGTA, 2 mM dithiothreitol, pH 6.8). After sonication and clarification, tau proteins were purified by boiling for 5 min followed by centrifugation and collection of the tau-containing soluble fraction. The purified proteins were separated by SDS-PAGE, transferred to nitrocellulose and the blots were incubated with anti-tau antibody (polyclonal, Sigma, St. Louis, MO, USA). The tau reactive bands

were visualized using ECL reagents (Amersham, Arlington Heights, IL, USA).

## 3. Results

### 3.1. Protein purification and Western blot analysis

Both wild-type and V337M mutant tau were expressed at detectable levels 48 h post-infection (p.i.), and were maximal at 80 h p.i. Purification of wild-type and V337M mutant tau infected cells yielded 10 pg of protein per cell with no consistent differences between wild-type and mutant cells. SDS-PAGE gel followed by Western blot analysis of the protein showed similar banding patterns for tau in each case. Three major bands were observed, corresponding to different phosphorylation states of the tau proteins.

### 3.2. Phase contrast appearance of Sf9 cells

Cells were infected with wild-type and the V337M tau containing viruses at identical titers. In both cases, formation of processes started 50–52 h p.i. Initially, a higher percentage of wild-type expressing cells showed processes when compared to those expressing the V337M tau mutation (data not shown), but at 72 h after infection the percentage of process bearing cells was equal in both cases (Fig. 1). There were no differences observed in the average number of processes per cell.

### 3.3. Ultrastructural analysis of microtubule organization

Electron micrographs of cross-sections of the processes revealed a highly ordered packing of microtubules in the wild-type tau-infected cells (Fig. 2A,B). The average distance between adjacent microtubules was  $13 \pm 3.9$  nm (Fig. 3A). In contrast, cells infected with the V337M tau mutation showed a much less organized cytoskeleton (Fig. 2C–E). In these cells, microtubule spacing varied widely. The microtubules were sometimes in close contact with each other. In other cases, they were separated by normal wild-type cross-bridge lengths, or by distances far larger than the average wild-type spacing. The mean intermicrotubular distance for the cells infected with V337M tau was  $17 \pm 7.9$  nm with a wider range of distributions than observed for wild-type tau (Fig. 3A). The difference between the two mean intermicrotubular distances is

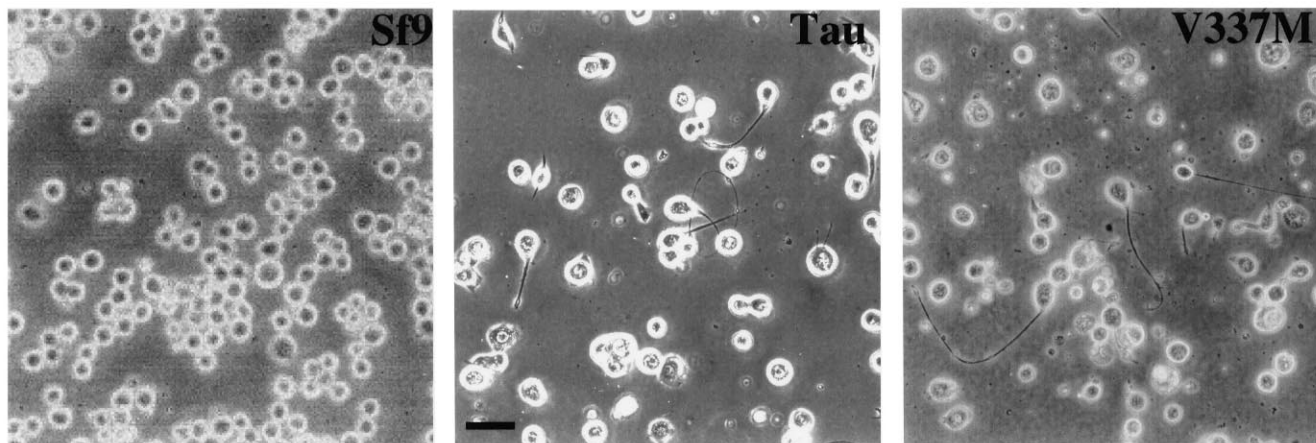


Fig. 1. Phase contrast of Sf9 cells. Phase microscope images of uninfected Sf9 cells (left panel), wild-type tau infected Sf9 cells (72 h p.i.) (middle panel), V337M tau infected cells (72 h p.i.) (right panel). Both wild-type tau and V337M tau infected cells grow processes, but no morphological differences can be seen between them at the light microscopy level. The bar is 50  $\mu$ m long.

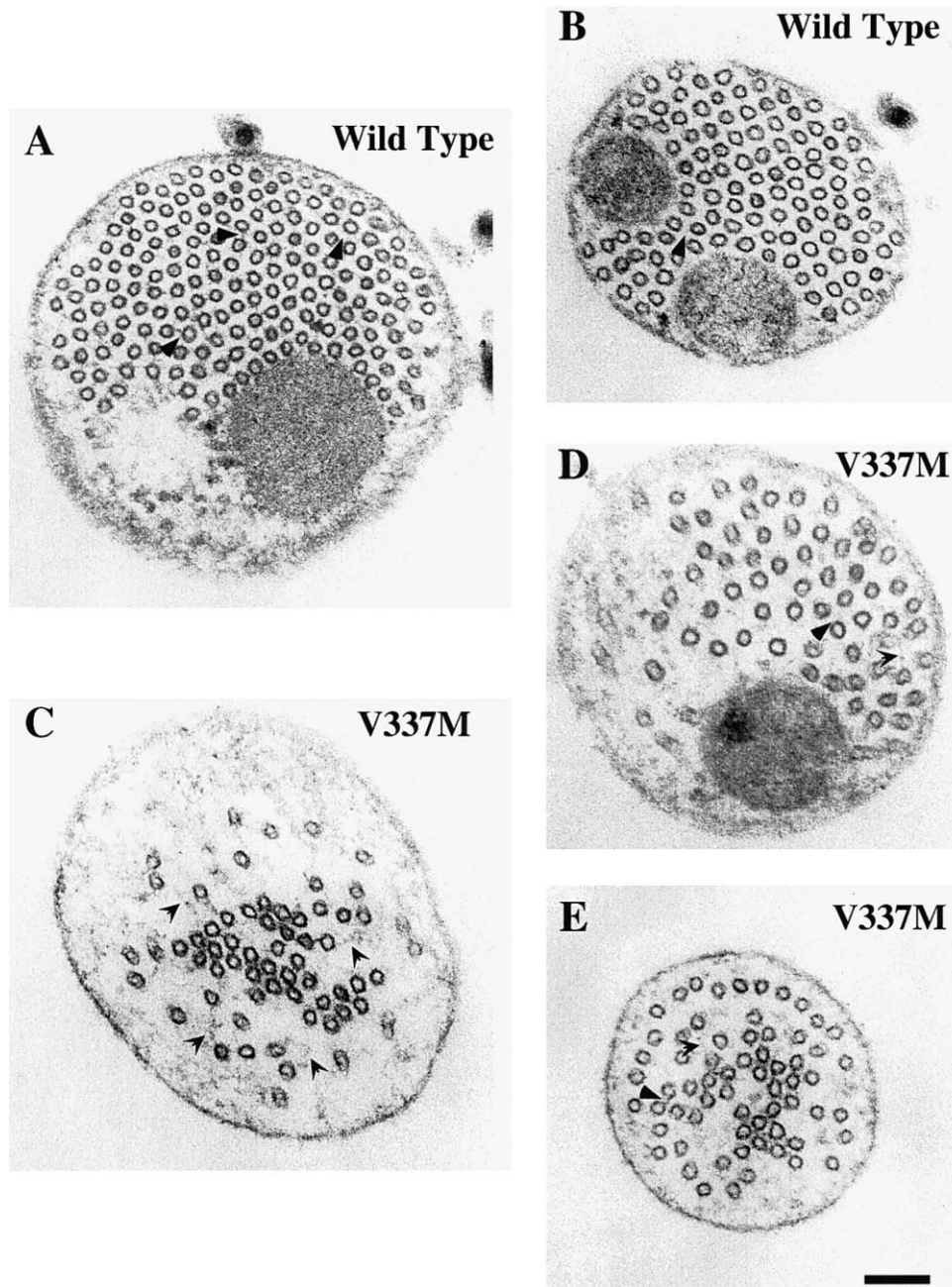


Fig. 2. EM analysis of wild-type and V337 M tau processes. Cross sectional views of processes induced by either wild-type tau recombinant viruses (A,B) or V337M tau recombinant viruses (C–E). Microtubules are well organized when the processes are induced by wild-type tau, whereas their organization is disrupted when they are induced by V337M tau. The differences in process diameter are due to variations in the distance of the sections from the cell body. The plain arrowheads show normal cross-bridges between microtubules, the barbed arrowheads point to extra long bridges. The bar is 100 nm long.

significant ( $P < 0.02$ ). We also determined the number of microtubules within 20 nm of an adjacent microtubule. In the wild-type tau-infected cells each individual microtubule was surrounded by an average of  $5.36 \pm 0.78$  microtubules, while in the V337M tau-infected cells each microtubule was surrounded by  $3.02 \pm 1.59$  microtubules (Fig. 3B). The difference is significant ( $P < 0.005$ ). The average number of microtubules per process was 81 for wild-type tau and 49 for the V337M tau mutation. Accordingly, the average density of microtubules was higher in processes induced by wild-type tau ( $0.07$  MT/100 nm<sup>2</sup>) than by the V337M tau mutation ( $0.026$  MT/100 nm<sup>2</sup>).

#### 4. Discussion

When wild-type or V337M tau are expressed in Sf9 cells, similar amounts of protein are synthesized in each case. However, mutant tau induces processes that form later, have fewer microtubules, have larger and more irregular intermicrotubule distances and have less regular microtubule packing than processes formed with wild-type tau. The relative lag in the formation of processes in the Sf9 cells expressing V337M tau could be related to the decreased efficiency of the V337M tau mutation in nucleating and/or stabilizing microtubule assembly which has been observed in vitro [15]. In particular, the

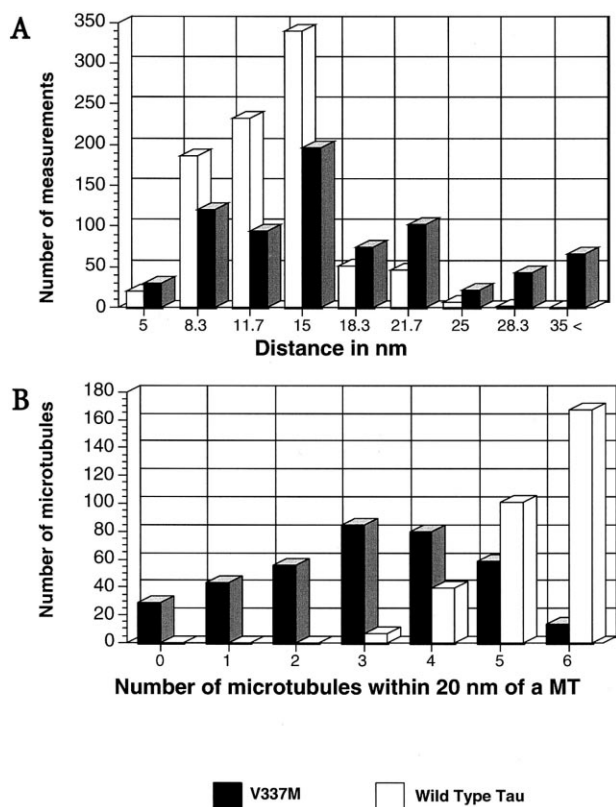


Fig. 3. Intermicrotubule distances and microtubular clustering. A: Distance distribution between the microtubules within the processes in wild-type and V337M tau. Black bars are V337M tau; white bars are wild-type tau. B: Relations of microtubules within the processes to one another. All the microtubules that fall within a 20 nm diameter from the outside wall of a given microtubule are counted. Black bars are V337M tau; white bars are wild-type tau.

V337M tau mutant shows an initial lag phase in microtubule polymerization which is twice as long as that induced by wild-type tau [15,16]. It could also be related to a mechanism in which coordinated polymerization of groups of microtubules favors process formation. The disorganization of the cytoplasm of the cellular processes in cells expressing the V337M tau when compared to wild-type tau could also be due to the lower affinity of V337M tau for microtubules [15].

Intermicrotubular spacing in the processes is regulated by the projection domain of tau [23]. The bridges between microtubules could be formed either by the interactions of the tau projection domains with adjacent microtubules, or by the binding of the tau projection domains to one another in an antiparallel manner. Studies in our laboratory have failed to find evidence for specific interactions of the projection domains with microtubules, while the antiparallel aggregation of tau results in paired helical filament formation in vitro [24]. In the antiparallel model, each cross-bridge would be dependent on a pair of tau molecules, one on each of the microtubules in the pair being in register with each other. Lowering the binding affinity of tau would result in more frequent failure of a tau molecule on one microtubule to find a tau molecule on an adjacent microtubule with which to pair. Since pairing must occur multiple times along the length of the tubule to maintain spacing, a decrease in the pairing of microtubules would lead to disorganization of the microtubule cytoskeleton. It is also possible that the disorga-

nization could reflect structural changes in tau itself [19]. The V337M mutation is just after the third repeat of the microtubule binding and distant from the projection fragment that regulates intermicrotubular spacing [23]. However, the mutation could alter the angle of tau attachment to tubulin leading to a change in the angle at which the projection fragment projects from the tubule. Such an alteration, though likely to be small in amplitude, could result in the microtubules being out of register with one another decreasing the probability of forming cross bridges.

It is difficult to know how closely the changes in the Sf9 cell model parallel those in the human brain. With the exception of the appearance of PHF and other tau aggregates, little is known about cytoskeletal organization in human brains carrying tau mutations. This is partially due to the poor preservation of microtubules in postmortem formalin fixed specimens. Even if preservation were not a problem, alterations in human tissue are likely to be subtle, since both wild-type and mutant tau are expressed.

The data presented here suggest that cytoskeletal disorganization and less than optimal cytoskeletal function can result from the V337M tau mutation. Over time this disorganization could result in one or more of the following: a greater energetic burden on the cell, the accumulation of oxidation products, a failure of retrograde transport of neurotrophic factors or problems in support of the synapse. Studies on each of these parameters will be required in both cell culture and animal models expressing mutant tau molecules to determine which, if any, of these mechanisms is involved.

*Acknowledgements:* This work was supported by grants from the NIH. N.S.L. and C.L.L. were supported in part on Training Grant AG00189.

## References

- [1] Migheli, A., Butler, M., Brown, K. and Shelanski, M.L. (1988) *J. Neurosci.* 8, 1846–1851.
- [2] Lee, G., Cowan, N. and Kirschner, M. (1988) *Science* 239, 285–288.
- [3] Lewis, S.A., Wang, D.H. and Cowan, N.J. (1988) *Science* 242, 936–939.
- [4] Flament, S., Delacourte, A., Verny, M., Hauw, J.J. and Javoy-Agid, F. (1991) *Acta Neuropathol.* 81, 591–596.
- [5] Morris, H.R., Janssen, J.C., Bandmann, O., Daniel, S.E., Rossor, M.N., Lees, A.J. and Wood, N.W. (1999) *J. Neurol. Neurosurg. Psychiatry* 66, 665–667.
- [6] Baker, M. et al. (1999) *Hum. Mol. Genet.* 8, 711–715.
- [7] Bennett, P. et al. (1998) *Neurology* 51, 982–985.
- [8] Goedert, M. et al. (1999) *Nature Med.* 5, 454–457.
- [9] Wilhelmsen, K.C., Lynch, T., Pavlou, E., Higgins, M. and Nygaard, T.G. (1994) *Am. J. Hum. Genet.* 55, 1159–1165.
- [10] Foster, N.L., Wilhelmsen, K., Sima, A.A., Jones, M.Z., D'Amato, C.J. and Gilman, S. (1997) *Ann. Neurol.* 41, 706–715.
- [11] Mirra, S.S. et al. (1999) *J. Neuropathol. Exp. Neurol.* 58, 335–345.
- [12] Morris, H.R. et al. (1999) *Ann. Neurol.* 45, 270–271.
- [13] Iijima, M. et al. (1999) *NeuroReport* 10, 497–501.
- [14] D'Souza, I., Poorkaj, P., Hong, M., Nochlin, D., Lee, V.M., Bird, T.D. and Schellenberg, G.D. (1999) *Proc. Natl. Acad. Sci. USA* 96, 5598–5603.
- [15] Hong, M., Zhukareva, V., Vogelsberg-Ragaglia, V., Wszolek, Z., Reed, L., Miller, B.I., Geschwind, D.H., Bird, T.D., McKeel, D., Goate, A., Morris, J.C., Wilhelmsen, K.C., Schellenberg, G.D., Trojanowski, J.Q. and Lee, V.M. (1998) *Science* 282, 1914–1917.
- [16] Hasegawa, M., Smith, M.J., Iijima, M., Tabira, T. and Goedert, M. (1999) *FEBS Lett.* 443, 93–96.

- [17] Arawaka, S., Usami, M., Sahara, N., Schellenberg, G.D., Lee, G. and Mori, H. (1999) *NeuroReport* 10, 993–997.
- [18] Nacharaju, P., Lewis, J., Easson, C., Yen, S., Hackett, J., Hutton, M. and Yen, S.H. (1999) *FEBS Lett.* 447, 195–199.
- [19] Jicha, G.A., Rockwood, J.M., Berenfeld, B., Hutton, M. and Davies, P. (1999) *Neurosci. Lett.* 260, 153–156.
- [20] Dayanandan, R. et al. (1999) *FEBS Lett.* 446, 228–232.
- [21] Summers, M.D. and Smith, G.E. (1987) *Texas Agricultural Experiment Station Bulletin* 1555.
- [22] Knops, J., Kosik, K.S., Lee, G., Pardee, J.D., Cohen-Gould, L. and McConlogue, L. (1991) *J. Cell Biol.* 114, 725–733.
- [23] Frappier, T.F., Georgieff, I.S., Brown, K. and Shelanski, M.L. (1994) *J. Neurochem.* 63, 2288–2294.
- [24] Wille, H., Drewes, G., Biernat, J., Mandelkow, E.M. and Mandelkow, E. (1992) *J. Cell Biol.* 118, 573–584.